International Journal of Advanced Research in Electronics and Communication Engineering (IJARECE)
Volume 3, Issue 2, February 2014

Theoretical Modeling Investigation and Numerical Simulation of Optical Dipole Antennas in Different Optical Transmission Regions

Ahmed Nabih Zaki Rashed[1*], and Osama A. Oraby[2]
[1,2]Electronics and Electrical Communications Engineering Department
Faculty of Electronic Engineering, Menouf 32951, Menoufia University, EGYPT

***Abstract*— This paper has presented the theoretical modeling investigation and numerical simulation of different optical dipole antennas in different optical transmission bands. We have taken into account the basic transmission characteristics of optical dipole antennas in the ultraviolet, visible and near infrared transmission regions over wide range of the affecting parameters. Antenna equivalent circuit of lumped elements such as Inductance, capacitance, antenna resistance and radiation resistance has deeply studied. Radiation and reflection antenna efficiencies, maximum power transfer to the antenna, antenna radiation intensity, antenna directivity, radiation pattern intensity and antenna gain are the major important design parameters which are taken into account in current research.**

***Index Terms*— Optical antennas, Ultraviolet region, Visible region, Near infrared region, Transmission characteristics, and Dipole antennas.**

I. INTRODUCTION

An optical antenna is a detector for electromagnetic radiation in the infrared and visible portion of the spectrum. Its metallic structure couples the incident radiation and creates currents that are rectified by a transducer element. It is well known that metals lose their conductivity at optical frequencies and become dispersive and lossy. While losses reduce the antenna quality, dispersion mainly makes the design process more demanding and both losses and dispersion limit the frequency range where a certain metal may be applied. Antennas have played an essential role since the very beginning of Electromagnetism. Even one of the simplest and first designs, the dipole antenna, is being used nowadays because of its easy implementation and characteristics. In telecom applications the need for larger and larger bandwidths has demanded the use of higher and higher frequencies of the supporting electromagnetic waves [1]. The use of high-frequency radio waves and the inclusion of microwave radiations improved the performance and capacity of the previous links. At the same time, the antenna design developed more sophisticated layouts that have been successfully applied. From our point of view, an important leap was done with the design of planar antennas structures. They can be fabricated with imprinting and thin-film technologies on an appropriate substrate. In the radio electric spectrum, the shrinking in wavelength has been associated with the downscaling of antenna structures. Fortunately, the available fabrication techniques and the good radiation-metal interaction have allowed the realization and demonstration of the devices at shorter and shorter wavelengths. However, before antennas could reach optical frequencies in a reliable and practical way, the use of semiconductor detectors made possible the development of reliable lightwave links in free space and along dielectric waveguides (optical fibres). These optical networks use the available detectors in the optical range mainly based on semiconductor technology [2]. The efforts to improve the performance of these detectors, and the positive results obtained from these efforts, have deprived the need to look back toward the antenna designs and make them work also in the optical band. Antennas are components to receive and transmit electromagnetic waves. Whereas antennas are primary devices in radio frequency applications for many years, the concept of optical antennas is relatively new. Analogously , optical antennas are components designed to transceive optical signals. The application range where optical antennas will be used is likely to become as wide as the one for the radio wave counterpart. Already an established application area for optical antennas is near-field optical microscopy and spectroscopy. There the antenna efficiently converts the energy of an incident electromagnetic wave to highly localized energy. The antenna concept is used to increase the signal strength and the resolution but also to influence the radiative decay rates of sample molecules.

The purpose of optical antennas is to convert the energy of free propagating radiation to localized energy, and vice versa. Although this is similar to what radio wave and microwave antennas do, optical antennas exploit the unique properties of metal microstructures, which behave as strongly coupled plasmas at optical frequencies. It is hoped that optical antennas can increase the efficiency of light-matter interactions in important applications, such as light-emitting devices, photovoltaics, and spectroscopy. Electromagnetic antennas, a key enabling technology for devices such as cellular phones and televisions, are mostly used in the radio-wave or microwave regime of the electromagnetic spectrum. At optical frequencies, on the contrary [3], electromagnetic fields are controlled by re-directing the wave fronts of propagating radiation by means of lenses, mirrors, and diffractive elements. Because this type of manipulation is based on the wave nature of electromagnetic fields, it cannot be used to control fields on the sub wavelength scale. In contrast, radio wave and microwave technology predominantly uses antennas to manipulate electromagnetic fields, controlling them on the subwavelength scale and interfacing efficiently between propagating radiation and localized fields. Recent research in micro-optics and plasmonics has generated considerable interest in optical antennas, and several current studies are exploring ways of translating established radio wave and microwave antenna theories into the optical frequency regime. The introduction of the antenna concept into the optical frequency regime will lead to new technological

ISSN: 2278 – 909X

applications [4], such as enhancing absorption cross-sections and quantum yields in photovoltaics, releasing energy efficiently from micro scale light emitting devices, boosting the efficiency of photochemical or photo physical detectors, and improving spatial resolution in optical microscopy [5].

II. Optical Dipole Antennas

To couple incident electromagnetic energy with small scale electronic devices, antennas have been utilized. The antennas achieve this coupling by localizing the incident radiation to dimensions smaller than the wavelength. The coupling mechanism between small scale electronic devices and antennas at radio and microwave frequencies has been well understood. A similar coupling mechanism is applicable between micro-antennas operating at optical frequencies and objects with feature dimensions below the diffraction limit.

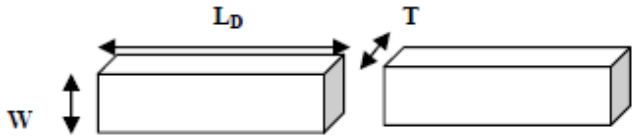

Fig. 1. Schematic view of optical dipole antenna and its dimensions.

At optical frequencies, microscale metallic antennas can be utilized to couple incident optical beams to length scales much smaller than the diffraction limit. A metallic dipole micro antenna, shown in Fig. 1 with dipole antenna length L_D, dipole antenna width W, and dipole antenna thickness T, primarily utilizes evanescent waves to couple electromagnetic energy to a sample in the near field. The direction of the polarization of the incident radiation and the antenna geometry play an important role in this process.

III. Antenna Modeling Analysis

High impedance circuits like liquid crystal displays, switched mode power supplies and fluorescent lamps that have small dimensions behave as electric dipoles. The ratio between voltage and current in such circuits is much larger than 377 Ω, the impedance of plane waves [6]. The emission is mainly determined by the dipole strength (the product of dipole length and dipole current; the latter being proportional to the signal voltage). The dipole length of most circuits is about equal to the distance between the two signal conductors. A voltage source connected in series with a short conductor (representing a capacitive load to the source) simulates an electric dipole [7]. The antenna can be represented by an equivalent circuit of several lumped elements such as a capacitance C, series inductance L, series antenna resistance R_A, and radiation resistance R_r and equivalent circuit of the antenna is connected to a voltage source Vs as shown in Fig. 2.

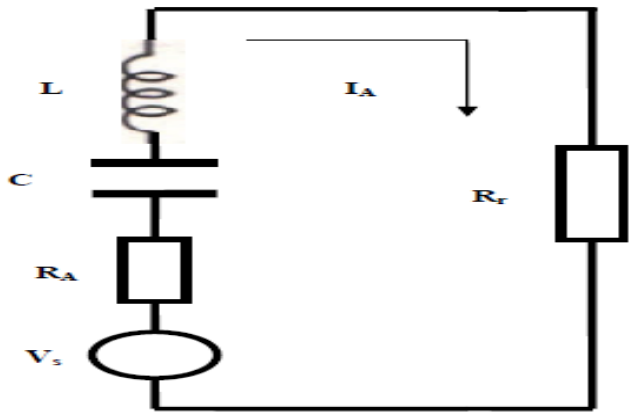

Fig. 2. Schematic view of an equivalent circuit of an antenna.

C represents the electric flux per unit of voltage and L the magnetic flux per unit of current; both depend on the length of the conductor and the current distribution along the dipole. For practical constructions, both the capacitance and inductance of the dipole antenna is given by [8]:

$$C = \frac{2\,\varepsilon_r \varepsilon_0\, L_D}{\pi}, \tag{1}$$

$$L = \frac{\mu_r \mu_0\, \lambda}{2\pi}, \tag{2}$$

Where ε_0=8.854x10^{-12} F/m is permittivity of free space μ_r is the relative permeability of the conductor material, ε_r is the relative permittivity of conductor material, and L_D is the length of one section of the dipole, μ_0 = 4πx10^{-7} H/m is permeability of free space, and λ is the operating optical signal wavelength. The current in a short conductor follows from the field strength E, the effective length L_{eff} and the distributed capacitance C between the two conductor sections. The voltage standing wave ratio (VSWR) can be expressed as the following formula [9]:

$$VSWR = \frac{|1+\Gamma|}{|1-\Gamma|}, \tag{3}$$

Where Γ is the reflection coefficient which is given by [10, 11]:

$$\Gamma = \frac{|R_A - Z_0|}{|R_A + Z_0|}, \tag{4}$$

Where Z_0 is the impedance of free space (≈120 π). And the return reflection loss is defined as [12]:

$$RL = -20\,\log|\Gamma|, \text{dB} \tag{5}$$

Where δ is the skin or penetration depth which is defined as [13]:

$$\delta = \left(\frac{\sqrt{2}\,\lambda}{2\pi c\sqrt{\mu\varepsilon}}\right)\left(\sqrt{1+\left(\frac{|\sigma|\lambda}{2\pi c\,\varepsilon}\right)^2}-1\right)^{-0.5} \tag{6}$$

Where c is the speed of light (3x10^8 m/sec), $\mu=\mu_0\mu_r$ is the permeability factor, $\varepsilon=\varepsilon_0\varepsilon_r$ is the permittivity factor, and σ is the material conductivity in S/m, which is given by the following relation [14, 15]:

$$|\sigma| = \frac{2\pi c\,\varepsilon_0}{\lambda}\left(\frac{1}{\varepsilon_r}-1\right), \tag{7}$$

In addition to the properties of the typical conductors materials based optical dipole antennas can be shown in Table 1.

ISSN: 2278 – 909X

Table 1. Properties of typical conducting materials based optical dipole antennas [12, 15, 18, 19].

Conductor material	Relative permeability, μ_r	Relative permittivity, ε_r
Copper (Cu)	0.96	1.0825
Gold (Au)	0.99	2.0222
Silver (Ag)	0.98	1.2656

Due to the mismatch at the antenna terminal, the reflection efficiency can be defined as the following formula [16]:

$$\eta_{ref} = \left(1 - |\Gamma|^2\right), \quad (8)$$

The antenna sheet resistance at the location of dipole at the source side can be [17]:

$$R_A = \frac{L_D}{|\sigma| T W}, \quad (9)$$

Where L_D is the dipole length, W is the dipole width, and T is the dipole thickness. Considering the effect of continuity at the end of the dipole, use triangular current distribution [18]:

$$R_r = 20\pi^2 \left(\frac{L_D}{\lambda}\right), \ \Omega \quad (10)$$

The antenna radiation efficiency can be expressed by the following formula:

$$\eta_r = \frac{R_r}{R_r + R_A}, \quad (11)$$

Therefore the total antenna efficiency is defined as [19]:

$$\eta_T = \eta_r \, \eta_{ref} \quad (12)$$

The maximum power transfer to the antenna can be expressed as [20]:

$$P_{Am} = \frac{0.125 |V_s|^2}{R_A + R_r}, \quad (13)$$

Assuming the conjugate matching conditions of maximum power transfer into an antenna with radiation resistance R_r and Loss less resistance (R_L=0), the maximum effective area is shown to be [10, 20]:

$$A_{em} = \frac{(E L_D)^2}{8\left(\frac{Z_0 E^2}{2(Z_0 + R_A + R_r)}\right)\left(\frac{80\pi^2 L_D^2}{\lambda^2}\right)}, \quad (14)$$

Where $E=V_s/L_D$ is the applied electric field to the antenna side. The radiation intensity of the dipole, U in Watt/μm^2 can be given by [11, 21]:

$$U = \frac{Z_0}{2}\left(\frac{I_A L_D}{2\lambda}\right)^2 \sin^2\theta \quad (15)$$

Where θ is the direction angle of electromagnetic waves, and $I_A=V_s/R_A+R_r$ is the dipole antenna current at resonance case. The antenna directivity and gain can be defined as the following expressions [21, 22]:

$$D = \frac{4\pi}{\lambda^2} A_{em}, \quad (16)$$

$$G_{dB} = 10 \log(\eta_r D), \quad (17)$$

IV. Numerical Results and Performance Analysis

Optical dipole antennas have been deeply investigated for dipole antennas in the visible and infrared spectrum regions to enhance it performance operation characteristics such as antenna gain, radiation intensity, maximum effective area and power transfer, antenna efficiency, and directivity over wide range of the affecting operating parameters as shown in Table 2.

Table 2. List of parameters used in this simulation for optical dipole antennas [3, 7, 9, 12, 18, 22].

Operating parameter	**Symbol**	**Value**
Operating signal wavelength (Ultraviolet region)	$\lambda_{Ultraviolet}$	$200 \le \lambda_{Ultraviolet}$, nm ≤ 400
Operating signal wavelength (Visible region)	$\lambda_{Visible}$	$400 \le \lambda_{Visible}$, nm ≤ 700
Operating signal wavelength (Near infrared region)	$\lambda_{Near\ infrared}$	$700 \le \lambda_{Near\ infrared}$, nm ≤ 1600
Dipole antenna length	L_D	$100 \le L_D$, nm ≤ 600
Dipole antenna width	W	$10 \le W$, nm ≤ 60
Dipole antenna thickness	T	$5 \le T$, nm ≤ 35
Source voltage	V_s	1.5 Volt [15]
Electromagnetic waves direction angle	θ	$0 \le \theta$, degree ≤ 360

Based on the modeling equations analysis over wide range of the operating parameters, and the series of the Figs. (3-36), the following features are assured:

i) Fig. 3 has assured that antenna circuit capacitance increases with increasing dipole antenna length for different antenna types under study. As well as gold antenna has presented the highest antenna circuit capacitance in comparison with other antennas under the same operation considerations.

ii) As shown in Fig. 4 has demonstrated that antenna circuit inductance increases with increasing operating optical signal wavelength in different optical transmission regions for different antenna types under study. As well as gold antenna has presented the highest antenna circuit inductance in comparison with other antennas under the same operation considerations.

iii) Figs. (5, 6) have indicated that antenna resistance increases with increasing both dipole antenna length and operating optical signal wavelength in different optical transmission regions for different antenna types under study. Moreover, the gold antenna has presented the lowest antenna resistance in comparison with other antennas under the same operation considerations in different optical transmission regions.

iv) Figs. (7-10) have proved that voltage standing wave ratio (VSWR) increases with increasing antenna thickness and decreasing antenna length for different antenna types under study considerations. As well as it is observed that in near infrared region (2'nd optical transmission window, λ=1300 nm, 3'rd optical transmission window, λ=1550 nm) has presented the lowest VSWR in comparison with other ultraviolet and visible optical transmission regions.

ISSN: 2278 – 909X

v) As shown in Figs. (11, 12) have assured that antenna radiation resistance increases with increasing dipole antenna length and decreasing operating optical signal wavelength in different optical transmission regions for different antenna types under study. Moreover, it is indicated that antenna radiation resistance in near infrared region (2'nd optical transmission window, λ=1300 nm, 3'rd optical transmission window, λ=1550 nm) has presented the lowest values in comparison with its values in other ultraviolet and visible optical transmission regions.

vi) Figs. (13, 14) have indicated that total antenna efficiency increases with increasing both antenna width and thickness and decreasing operating optical signal wavelength for different antenna types under study considerations. Gold antenna has presented the highest total antenna efficiency in comparison with other antennas under the same operating conditions.

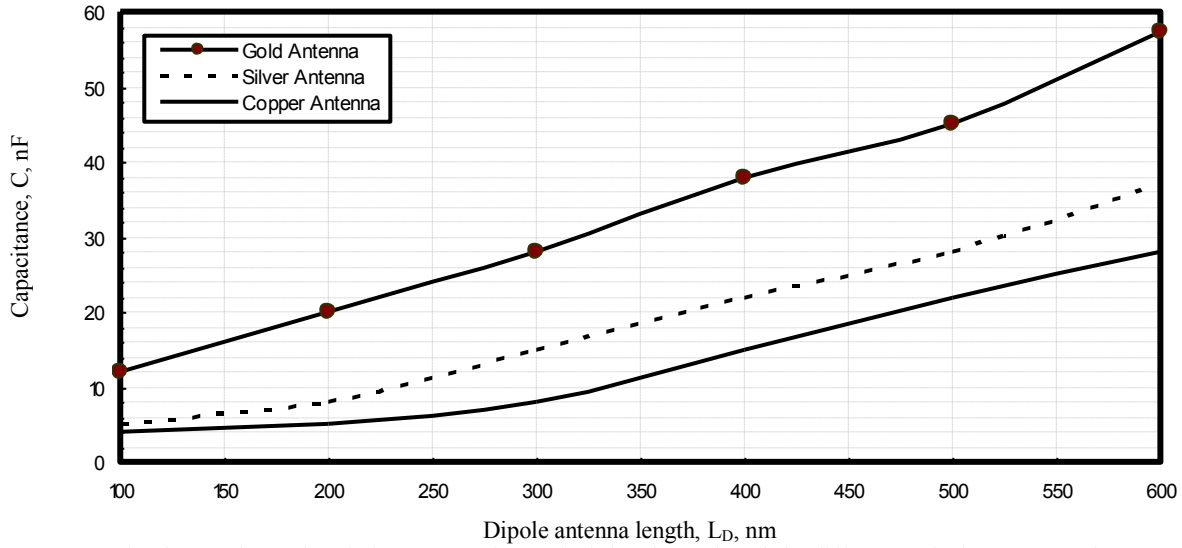

Fig. 3. Antenna circuit capacitance in relation to operating optical signal wavelength for different optical antennas at the assumed set of the operating parameters.

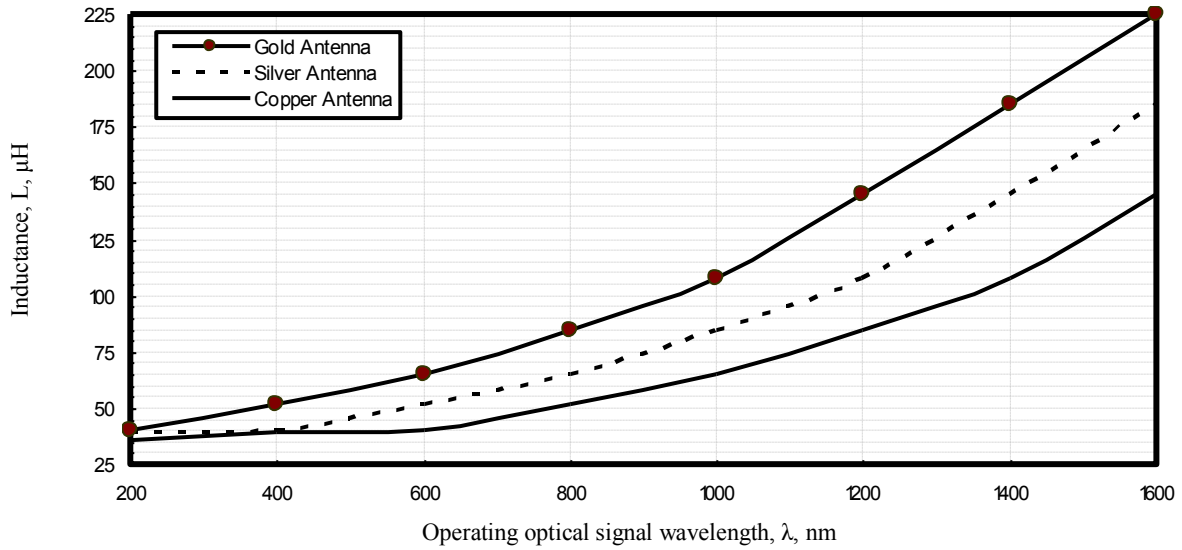

Fig. 4. Antenna circuit inductance in relation to operating optical signal wavelength for different optical antennas at the assumed set of the operating parameters.

ISSN: 2278 – 909X

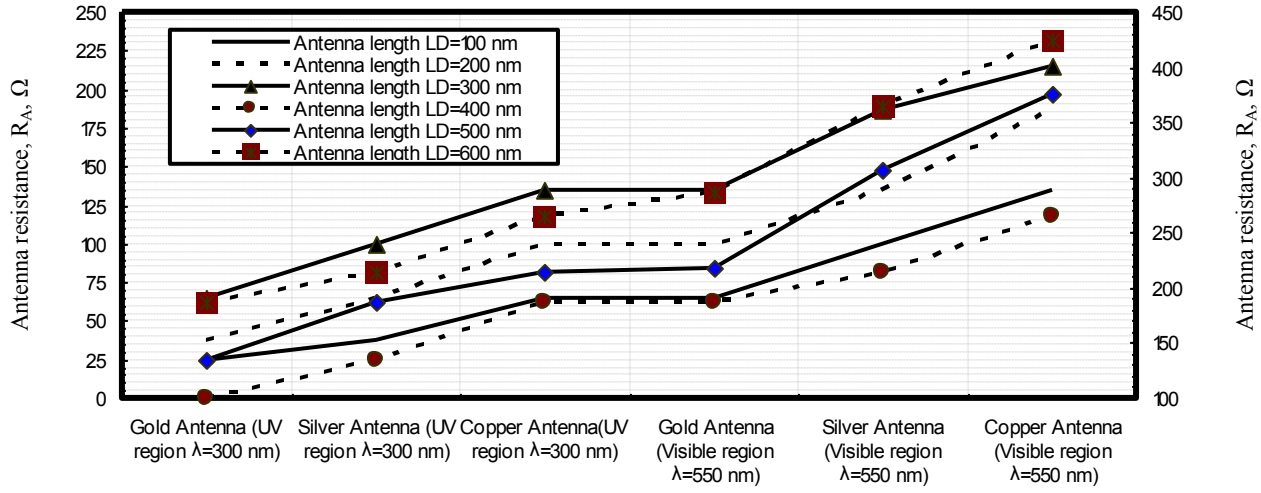

Fig. 5. Antenna circuit resistance in relation to different optical antenna types and lengths with ultraviolet and visible transmission regions at the assumed set of the operating parameters.

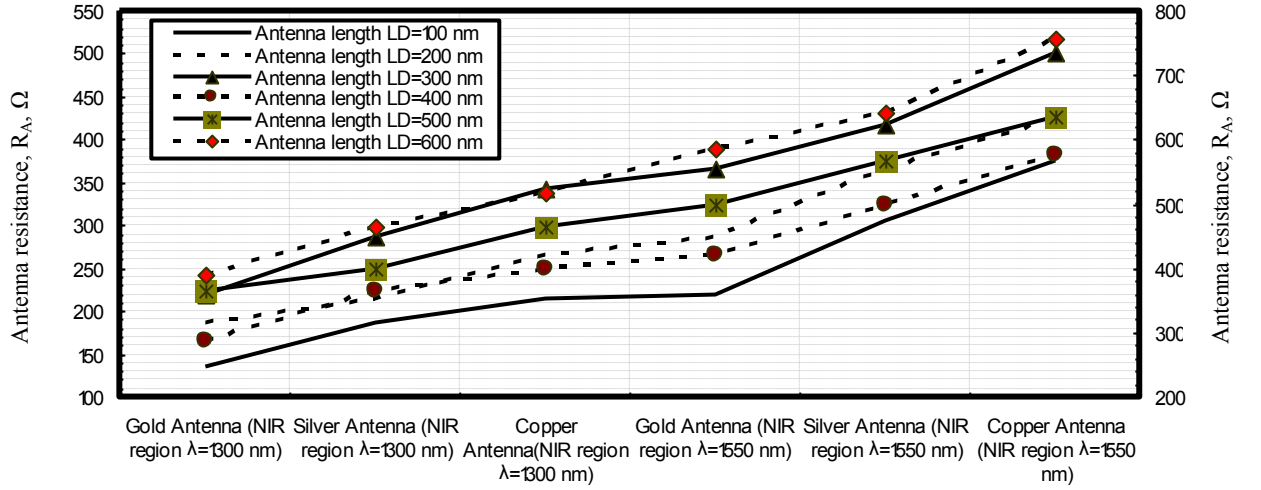

Fig. 6. Antenna circuit resistance in relation to different optical antenna types and lengths with near infrared transmission regions at the assumed set of the operating parameters.

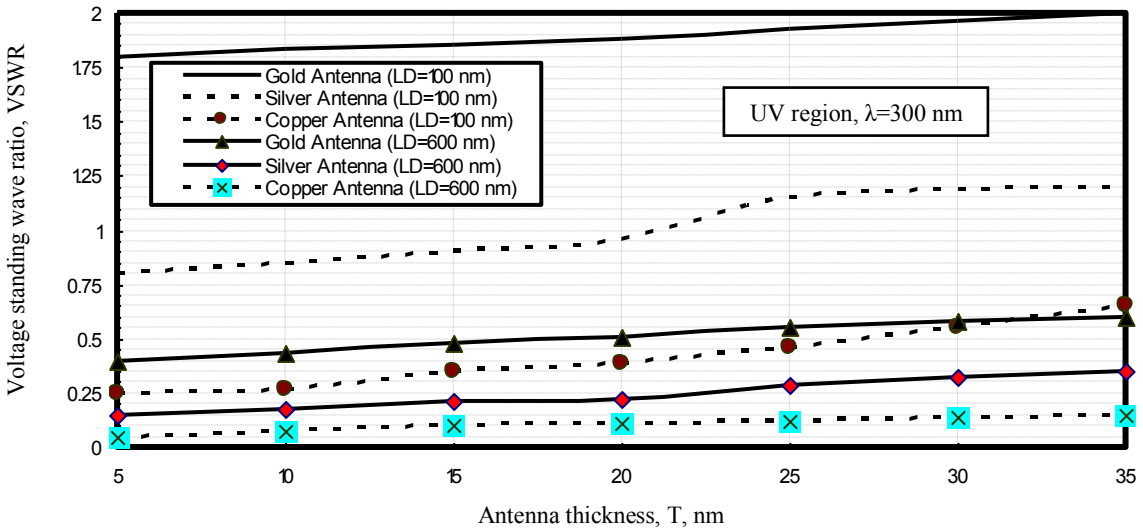

Fig. 7. Voltage standing wave ratio in relation to different optical antenna types, thickness and lengths with ultraviolet transmission region (λ=300 nm) at the assumed set of the operating parameters.

ISSN: 2278 – 909X

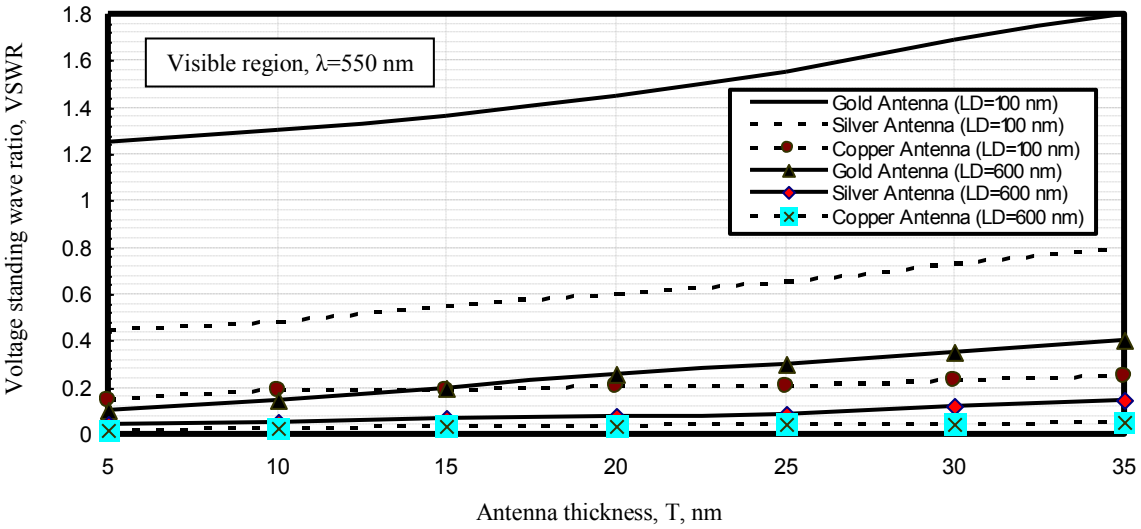

Fig. 8. Voltage standing wave ratio in relation to different optical antenna types, thickness and lengths with visible transmission region (λ=550 nm) at the assumed set of the operating parameters.

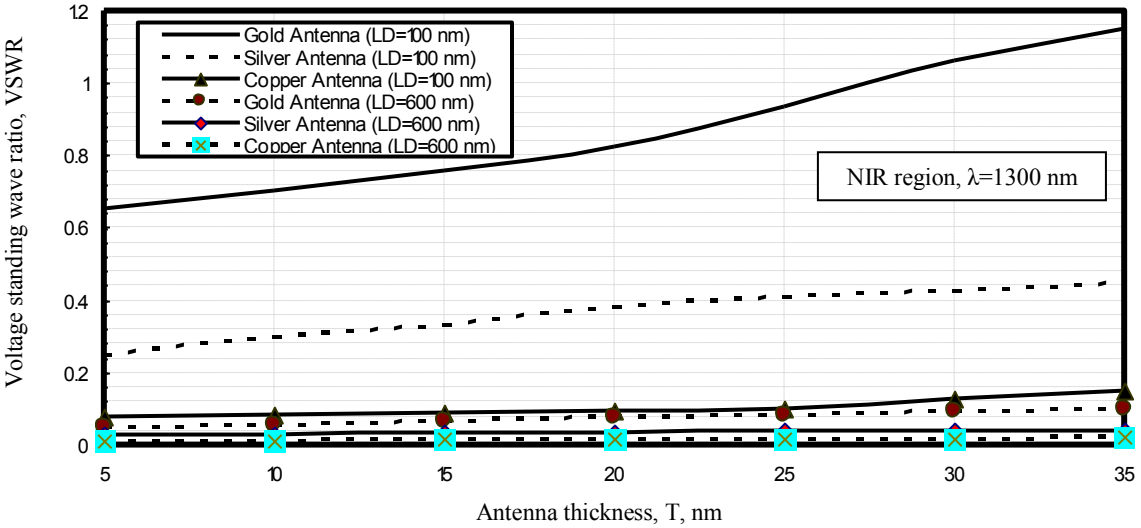

Fig. 9. Voltage standing wave ratio in relation to different optical antenna types, thickness and lengths with near infrared transmission region (λ=1300 nm) at the assumed set of the operating parameters.

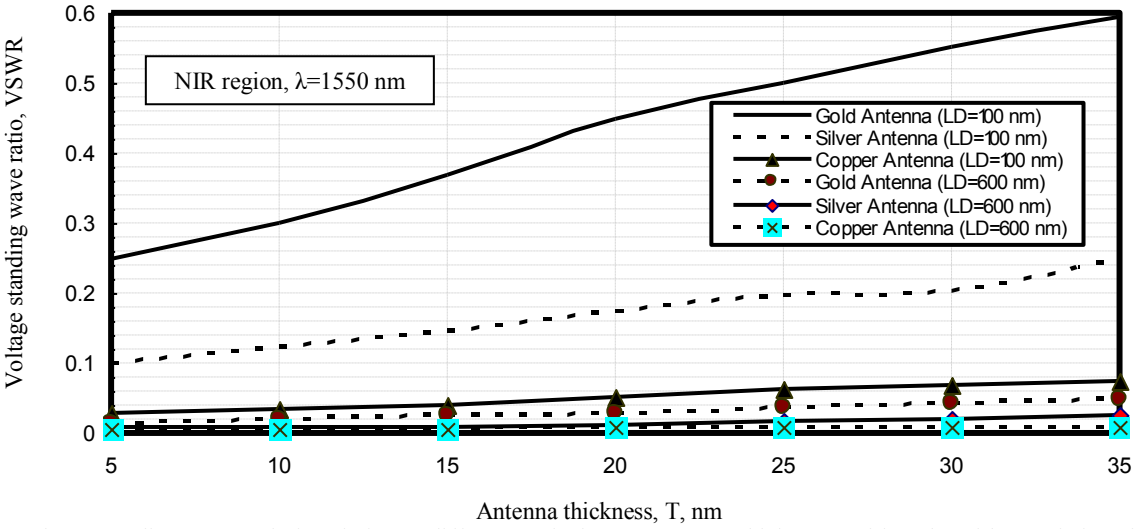

Fig. 10. Voltage standing wave ratio in relation to different optical antenna types, thickness and lengths with near infrared transmission region (λ=1550 nm) at the assumed set of the operating parameters.

ISSN: 2278 – 909X

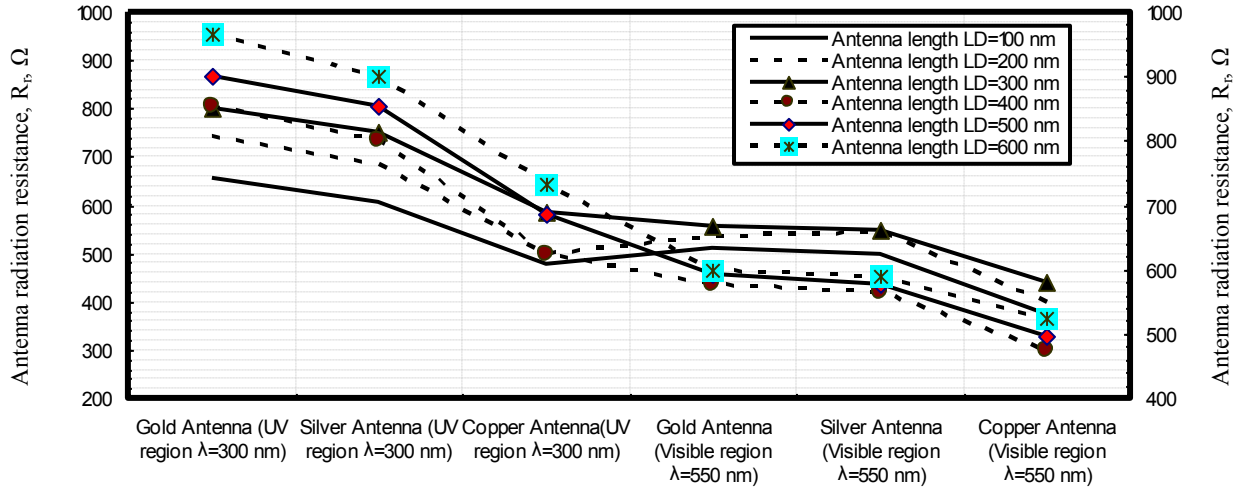

Fig. 11. Antenna radiation resistance in relation to different optical antenna types and lengths with ultraviolet and visible transmission regions at the assumed set of the operating parameters.

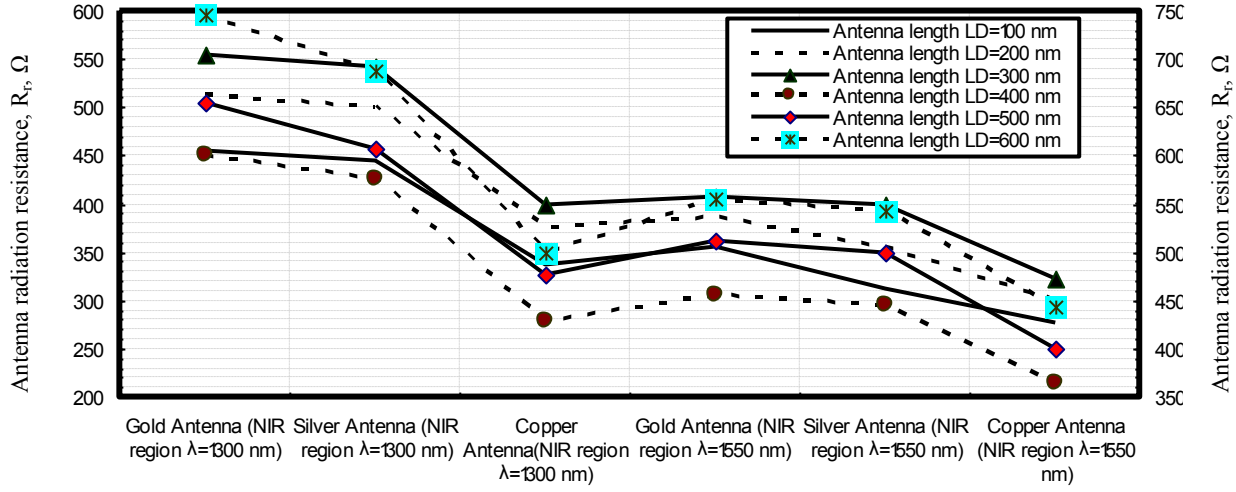

Fig. 12. Antenna radiation resistance in relation to different optical antenna types and lengths with near infrared transmission regions at the assumed set of the operating parameters.

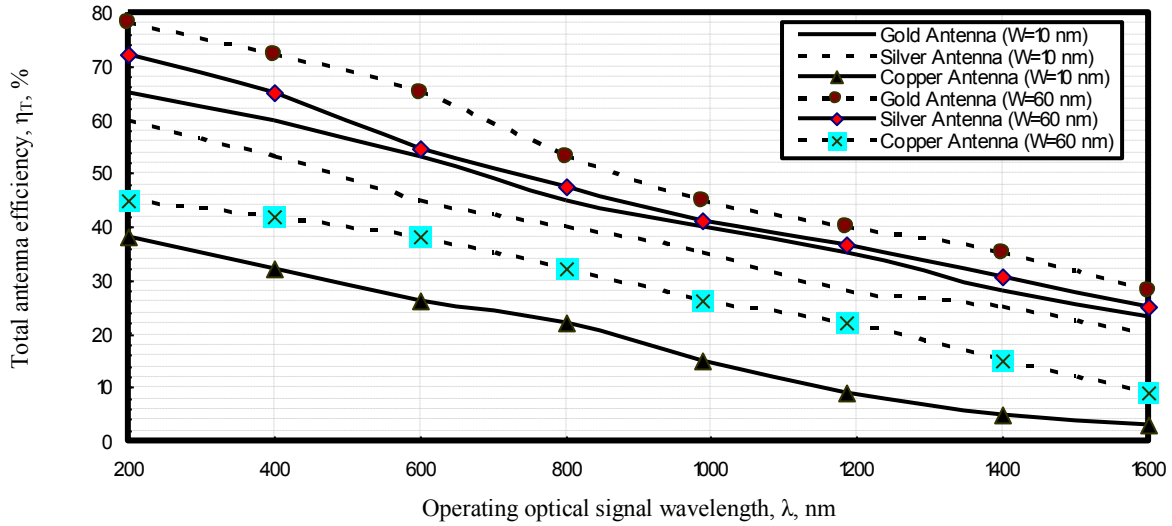

Fig. 13. Variations of total antenna efficiency against variations of operating optical signal wavelength and antenna width for different antenna types at the assumed set of the operating parameters.

ISSN: 2278 – 909X

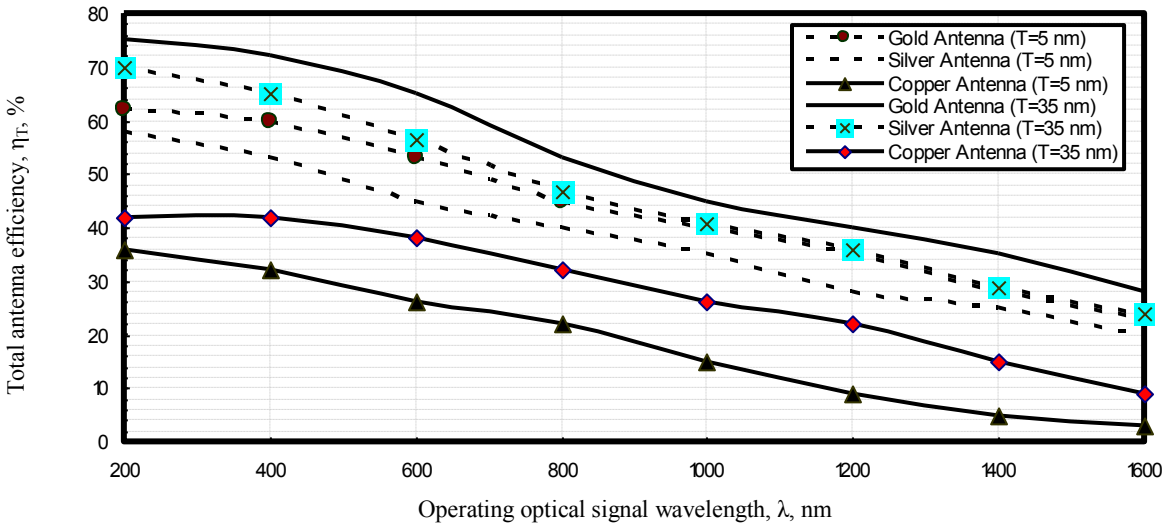

Fig. 14. Variations of total antenna efficiency against variations of operating optical signal wavelength and antenna thickness for different antenna types at the assumed set of the operating parameters.

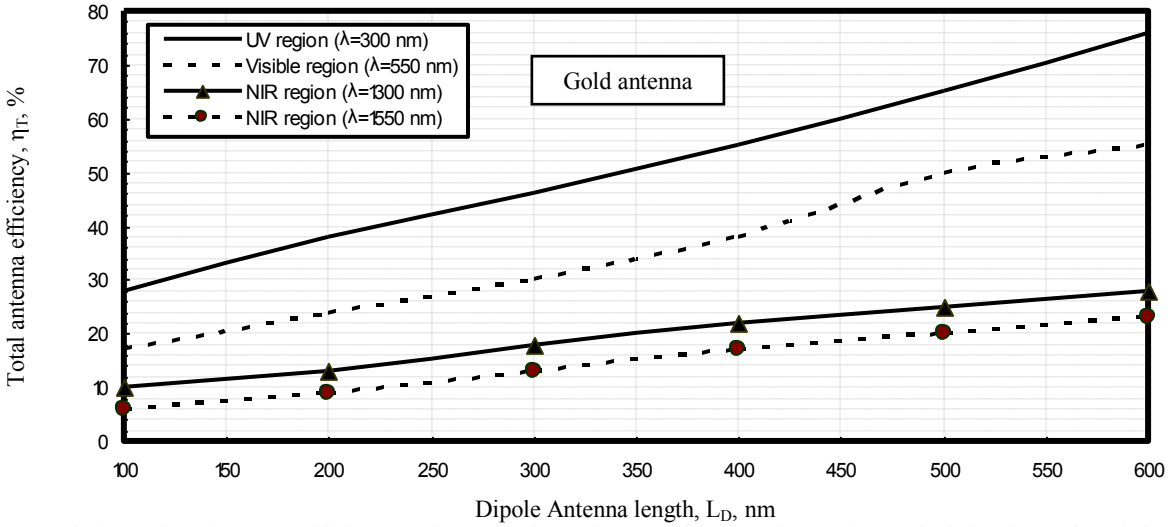

Fig. 15. Variations of total antenna efficiency against variations of antenna length and operating optical signal wavelength for gold antenna at the assumed set of the operating parameters.

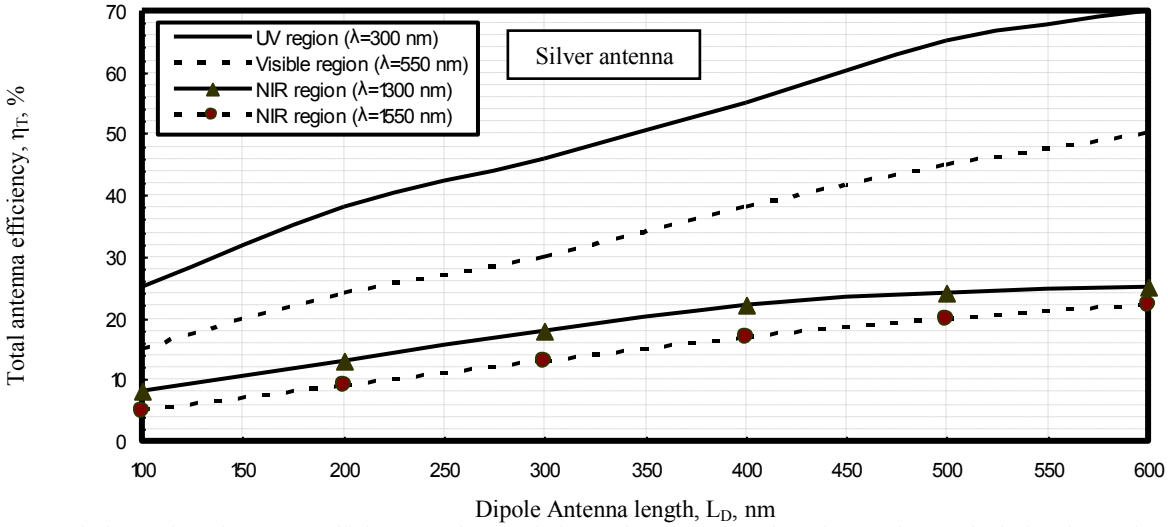

Fig. 16. Variations of total antenna efficiency against variations of antenna length and operating optical signal wavelength for silver antenna at the assumed set of the operating parameters.

ISSN: 2278 – 909X

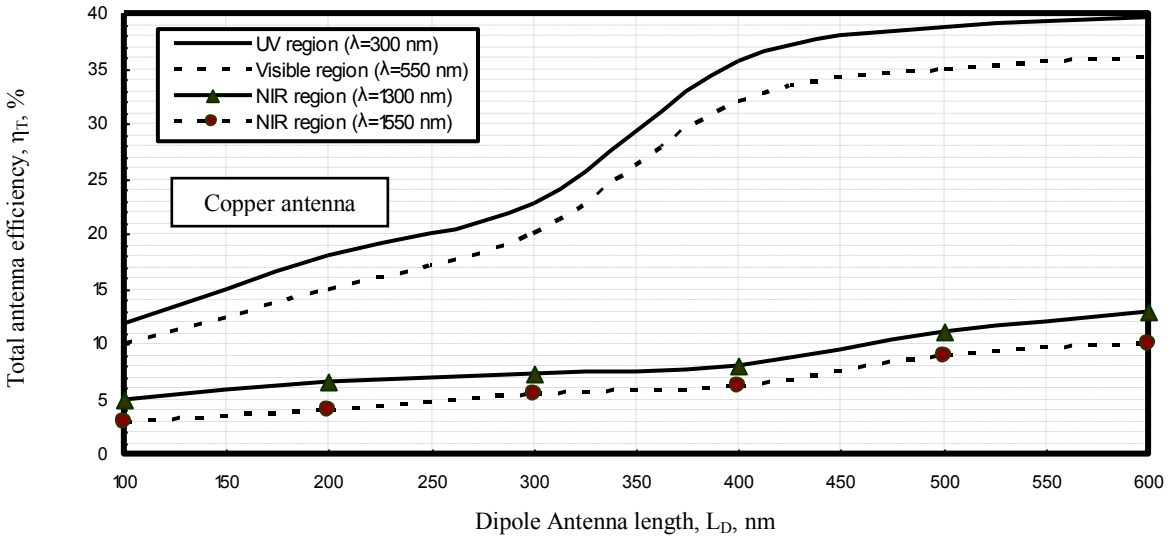

Fig. 17. Variations of total antenna efficiency against variations of antenna length and operating optical signal wavelength for copper antenna at the assumed set of the operating parameters.

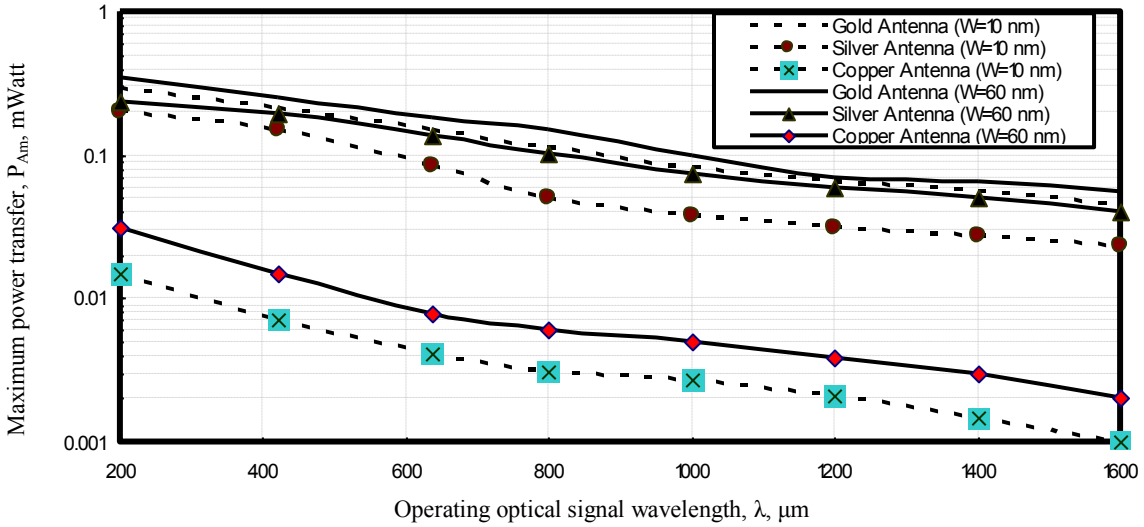

Fig. 18. Maximum power transfer in relation to operating optical signal wavelength and antenna width for different antenna types at the assumed set of the operating parameters.

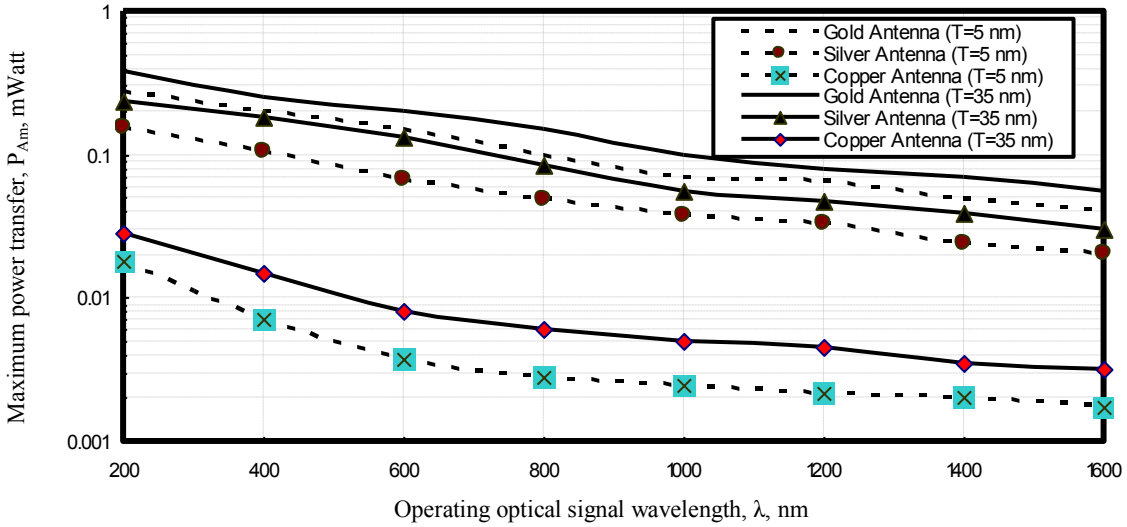

Fig. 19. Maximum power transfer in relation to operating optical signal wavelength and antenna thickness for different antenna types at the assumed set of the operating parameters.

ISSN: 2278 – 909X

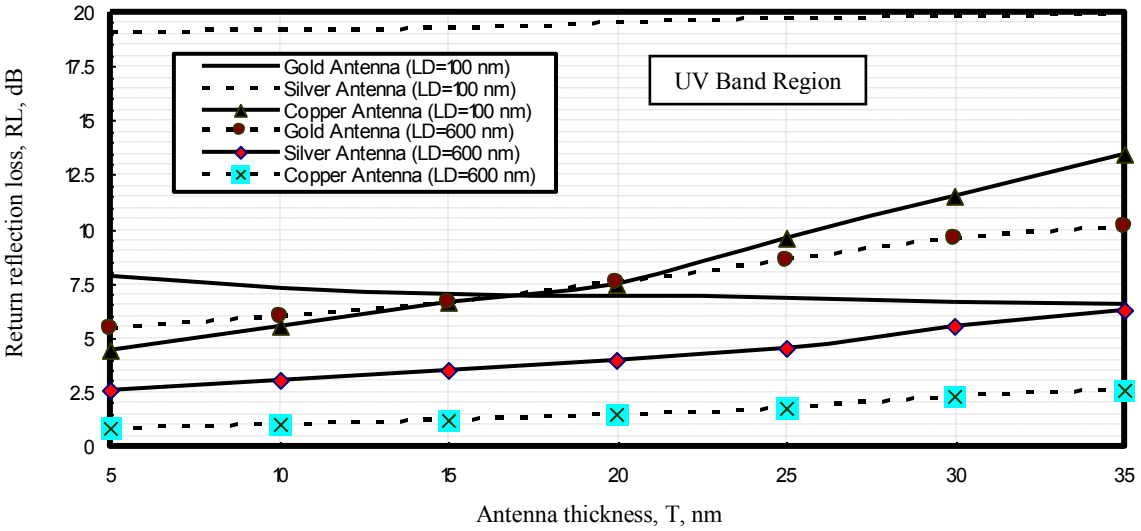

Fig. 20. Return reflection loss in relation to antenna thickness and length (antenna dimensions) for different antenna types in the ultra-violent band transmission region at the assumed set of the operating parameters.

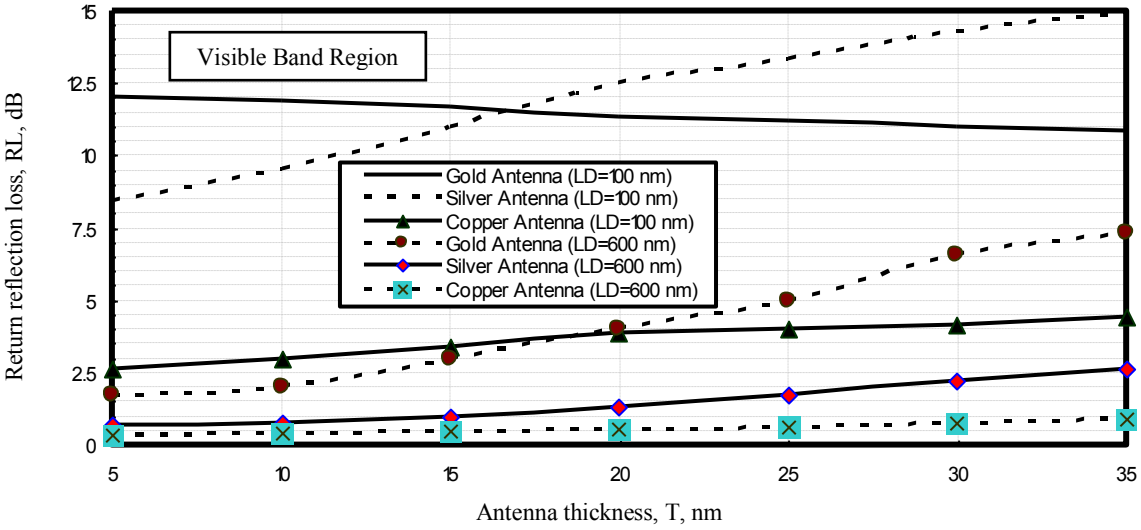

Fig. 21. Return reflection loss in relation to antenna thickness and length (antenna dimensions) for different antenna types in the visible band transmission region at the assumed set of the operating parameters.

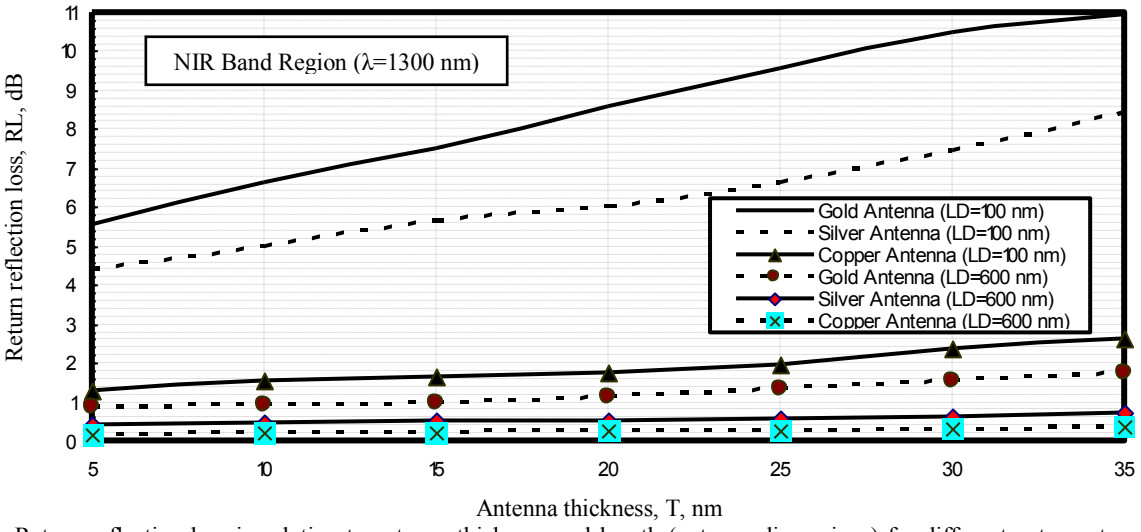

Fig. 22. Return reflection loss in relation to antenna thickness and length (antenna dimensions) for different antenna types in the near infrared band transmission region (λ=1300 nm) at the assumed set of the operating parameters.

ISSN: 2278 – 909X

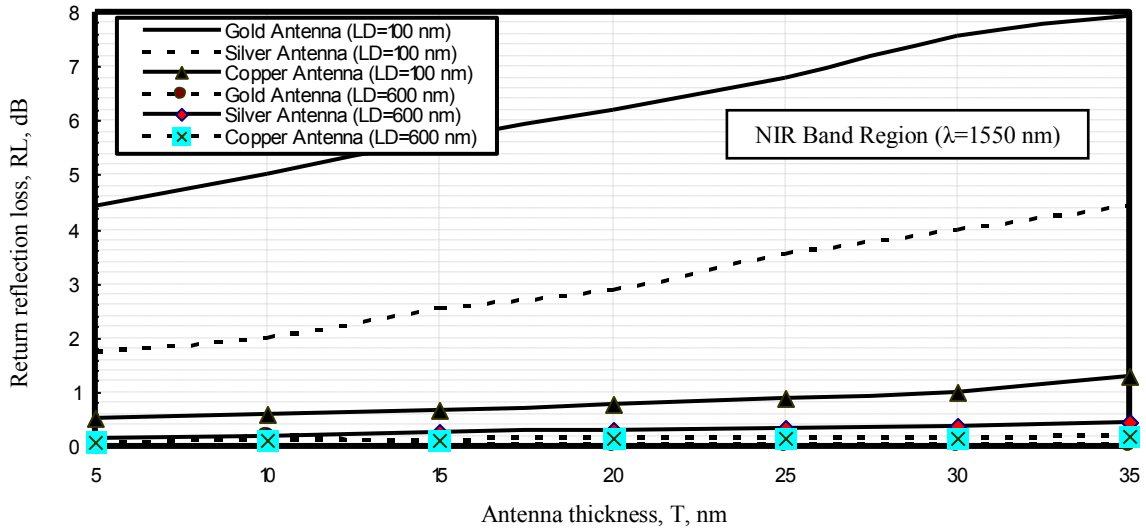

Fig. 23. Return reflection loss in relation to antenna thickness and length (antenna dimensions) for different antenna types in the near infrared band transmission region (λ=1550 nm) at the assumed set of the operating parameters.

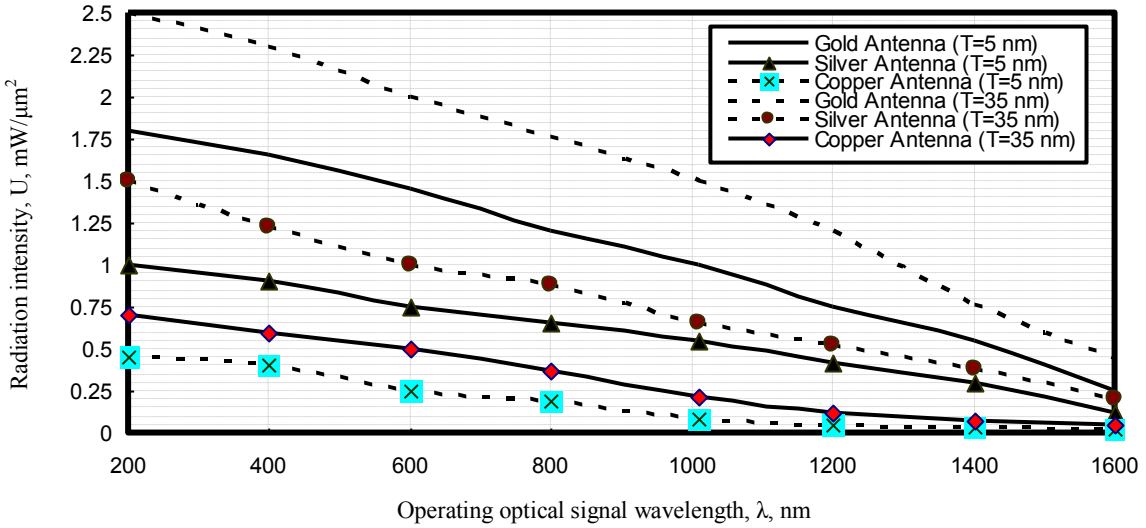

Fig. 24. Radiation intensity in relation to operating optical signal wavelength and antenna thickness for different antenna types at the assumed set of the operating parameters.

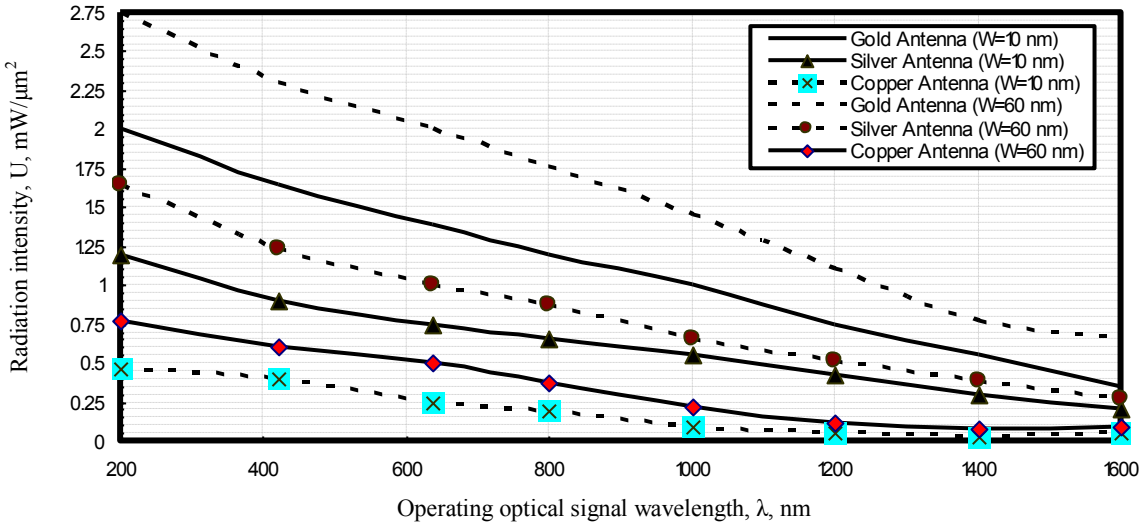

Fig. 25. Radiation intensity in relation to operating optical signal wavelength and antenna width for different antenna types at the assumed set of the operating parameters.

ISSN: 2278 – 909X

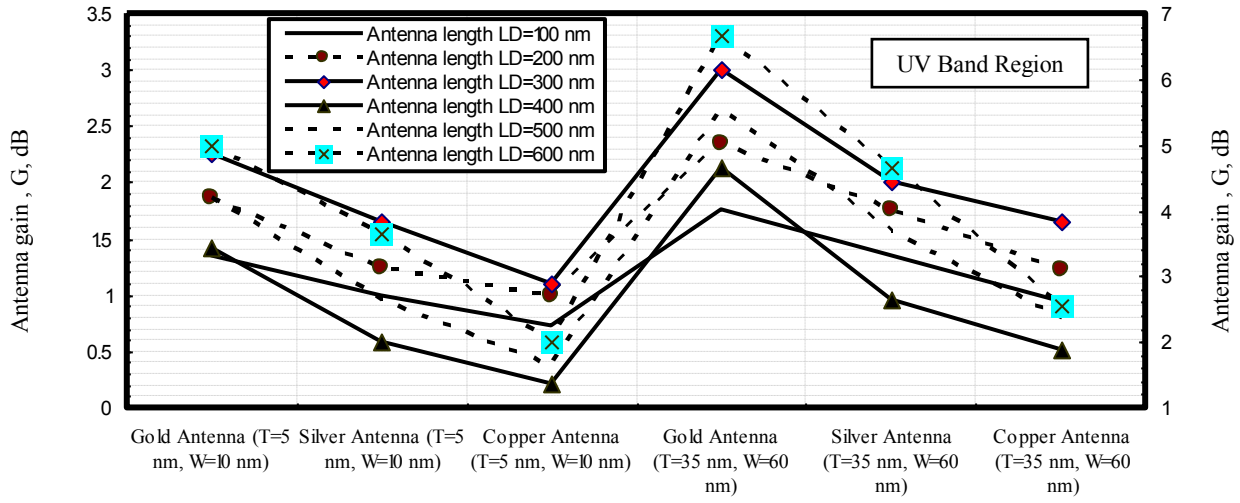

Fig. 26. Antenna gain in relation to different optical antenna types and lengths with ultra violet transmission region at the assumed set of the operating parameters.

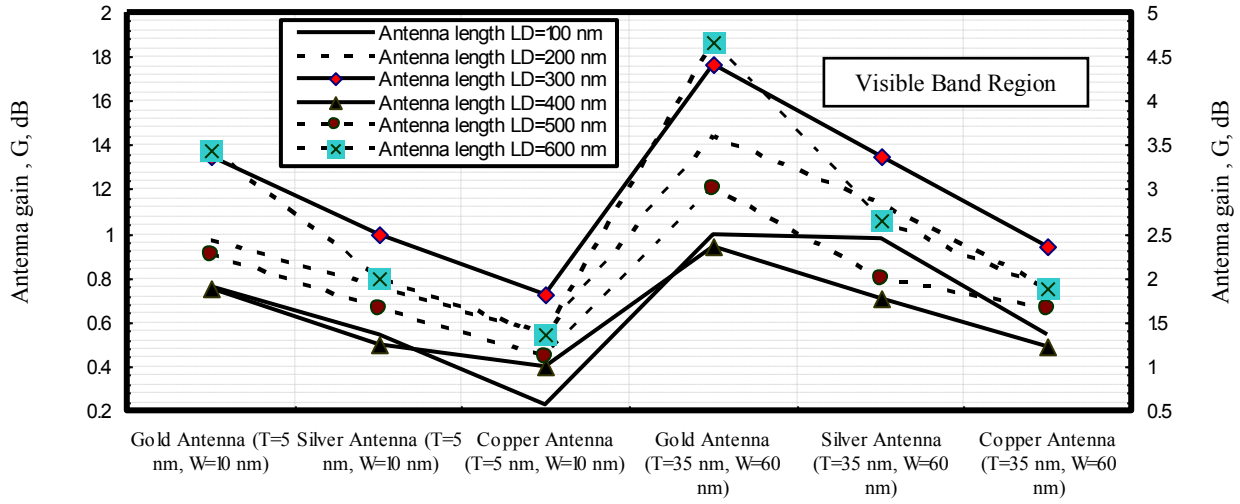

Fig. 27. Antenna gain in relation to different optical antenna types and lengths with visible transmission region at the assumed set of the operating parameters.

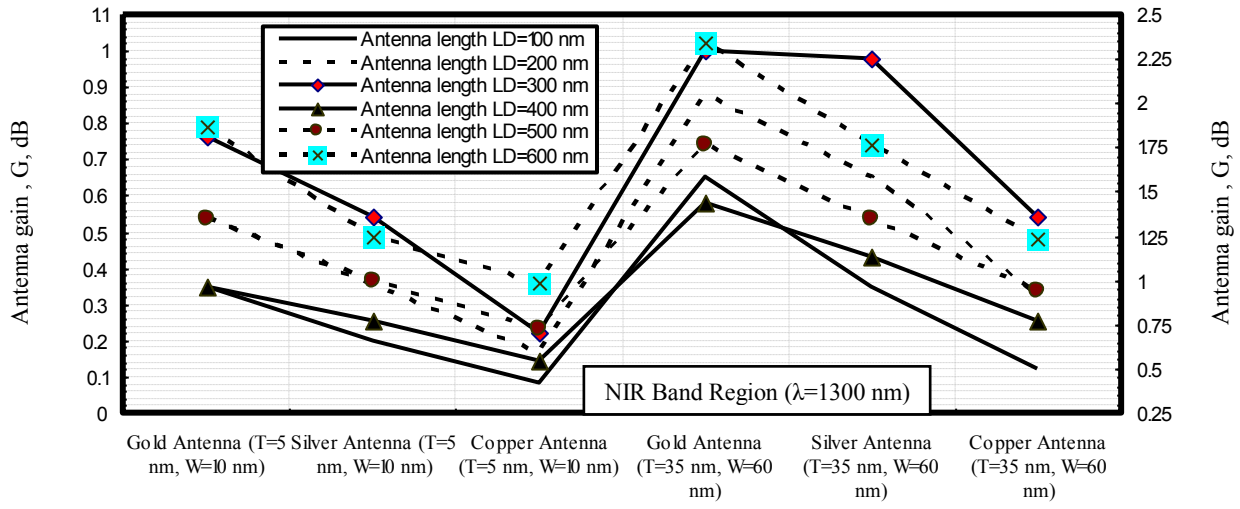

Fig. 28. Antenna gain in relation to different optical antenna types and lengths with near infrared transmission region (λ=1300 nm) at the assumed set of the operating parameters.

ISSN: 2278 – 909X

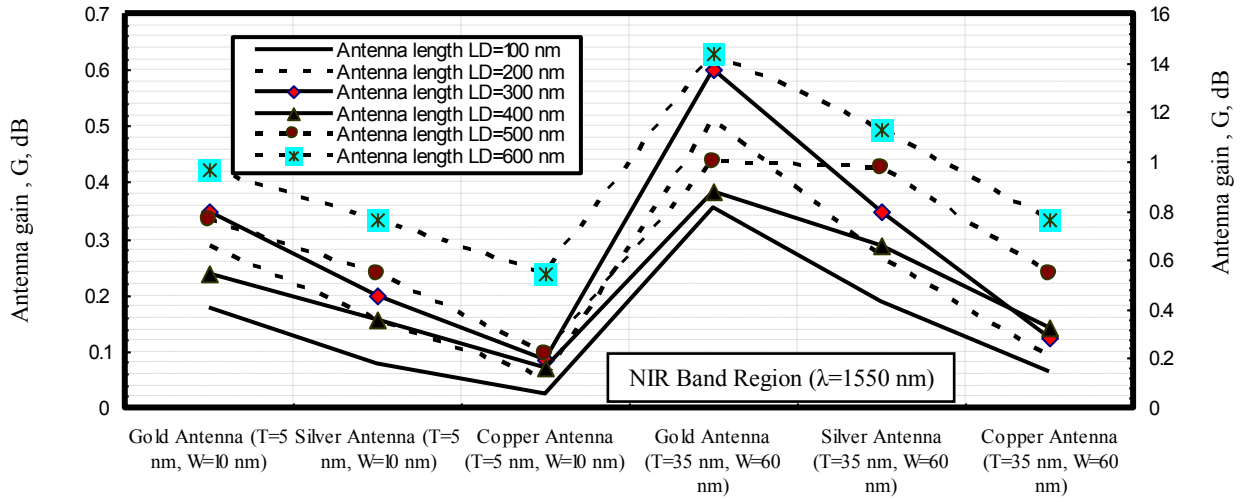

Fig. 29. Antenna gain in relation to different optical antenna types and lengths with near infrared transmission region (λ=1550 nm) at the assumed set of the operating parameters.

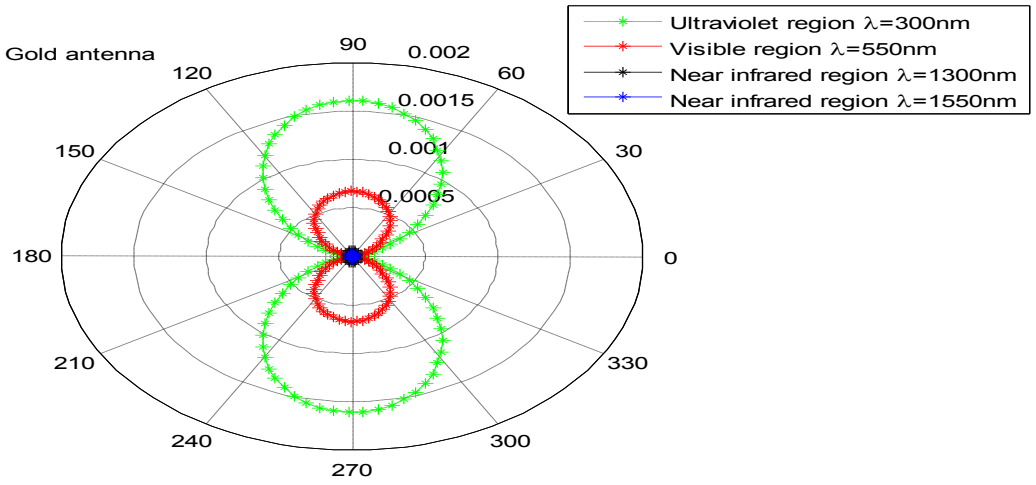

Fig. 30. Gold antenna radiation pattern intensity in relation to direction angle of electromagnetic waves and different optical transmission regions at the assumed set of the operating parameters.

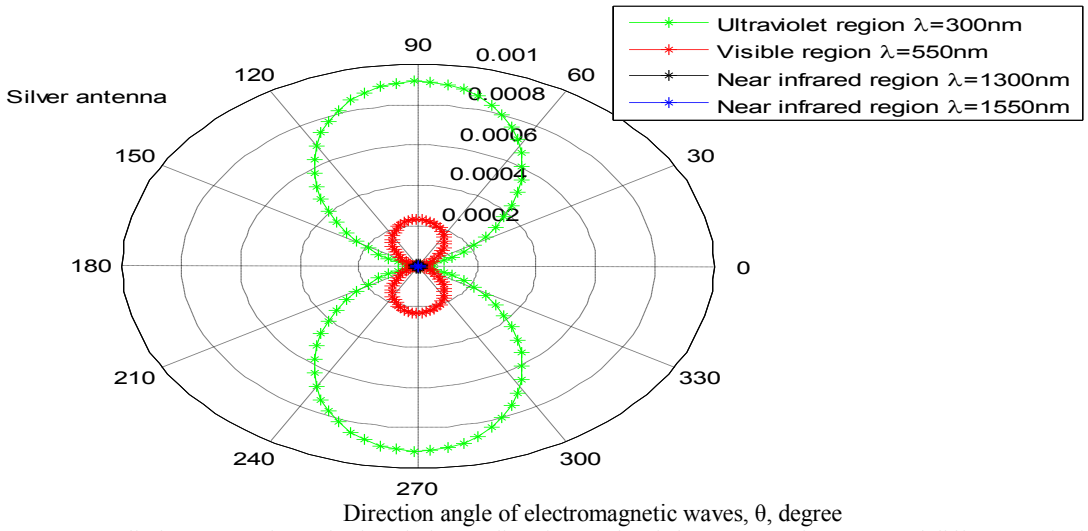

Fig. 31. Silver antenna radiation pattern intensity in relation to direction angle of electromagnetic waves and different optical transmission regions at the assumed set of the operating parameters.

ISSN: 2278 – 909X

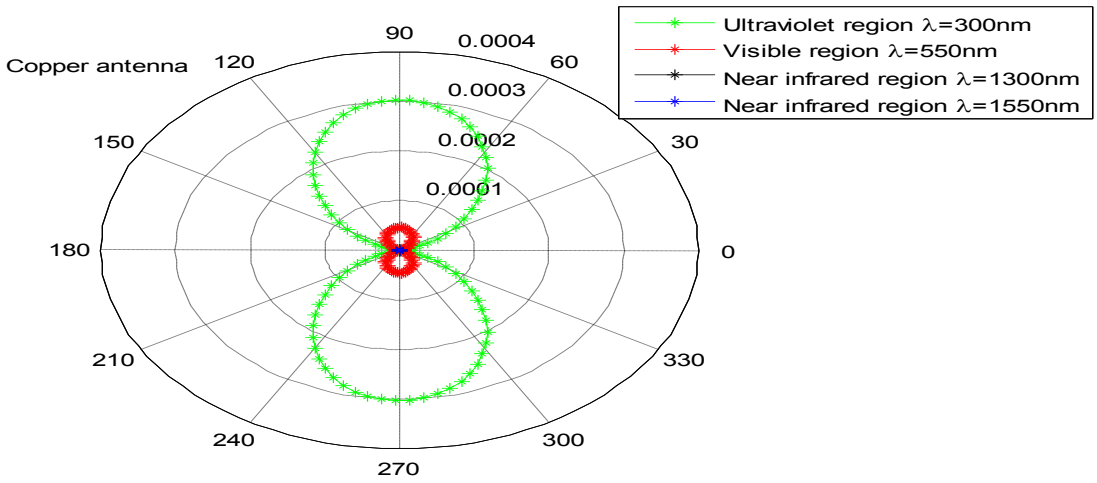

Direction angle of electromagnetic waves, θ, degree

Fig. 32. Copper antenna radiation pattern intensity in relation to direction angle of electromagnetic waves and different optical transmission regions at the assumed set of the operating parameters.

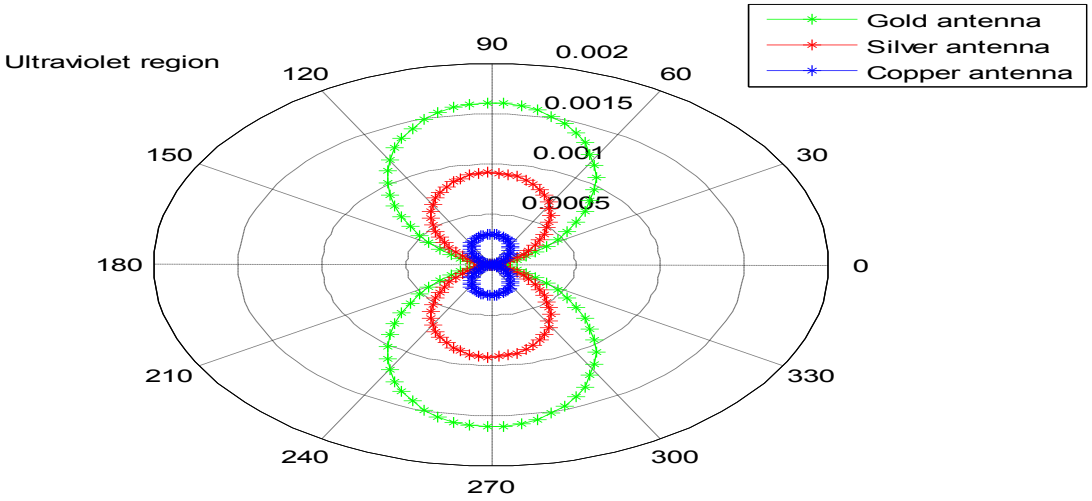

Direction angle of electromagnetic waves, θ, degree

Fig. 33. Antenna radiation pattern intensity in relation to direction angle of electromagnetic waves and different optical antenna types in ultraviolet transmission region at the assumed set of the operating parameters.

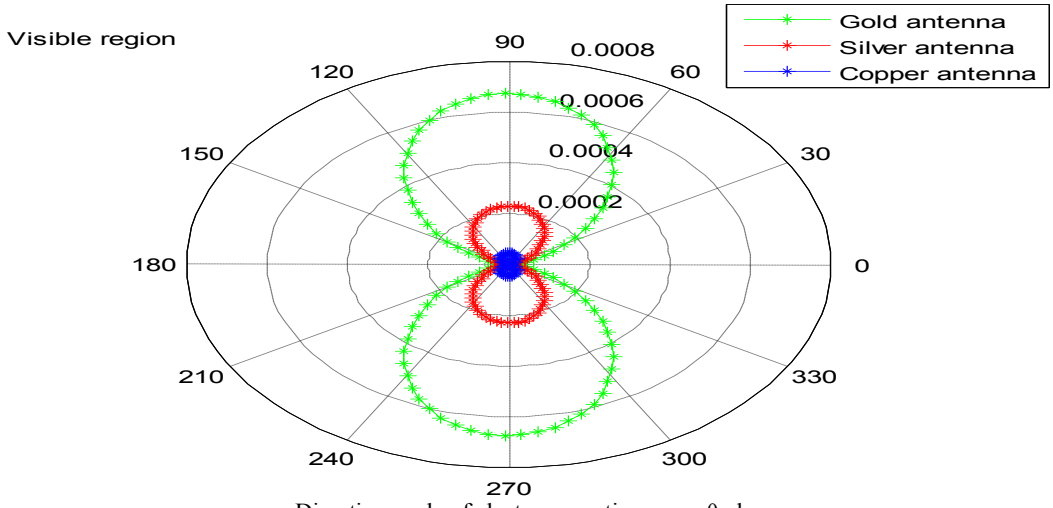

Direction angle of electromagnetic waves, θ, degree

Fig. 34. Antenna radiation pattern intensity in relation to direction angle of electromagnetic waves and different optical antenna types in visible transmission region at the assumed set of the operating parameters.

ISSN: 2278 – 909X

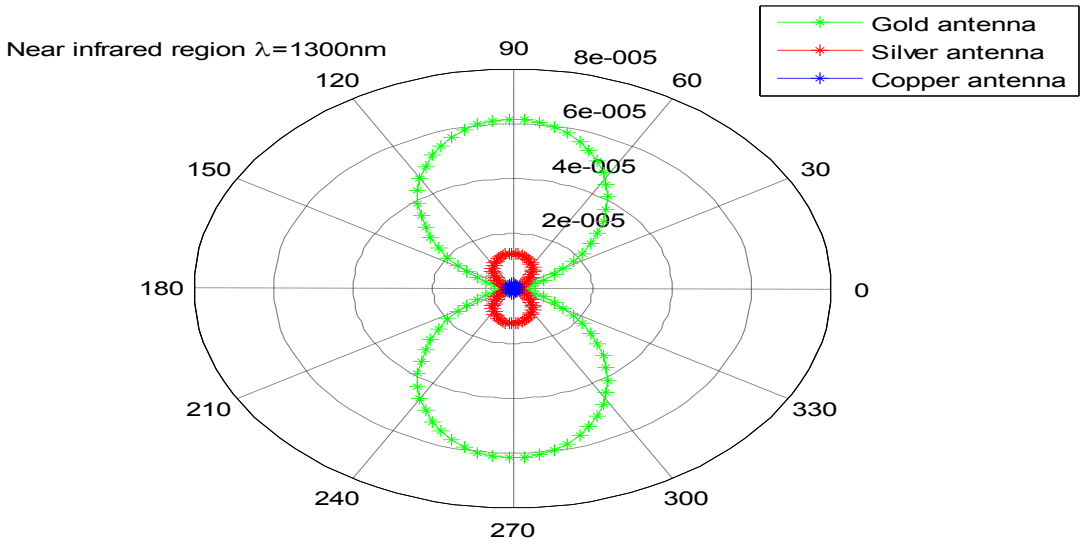

Fig. 35. Antenna radiation pattern intensity in relation to direction angle of electromagnetic waves and different optical antenna types in near infrared transmission region (λ=1300 nm) at the assumed set of the operating parameters.

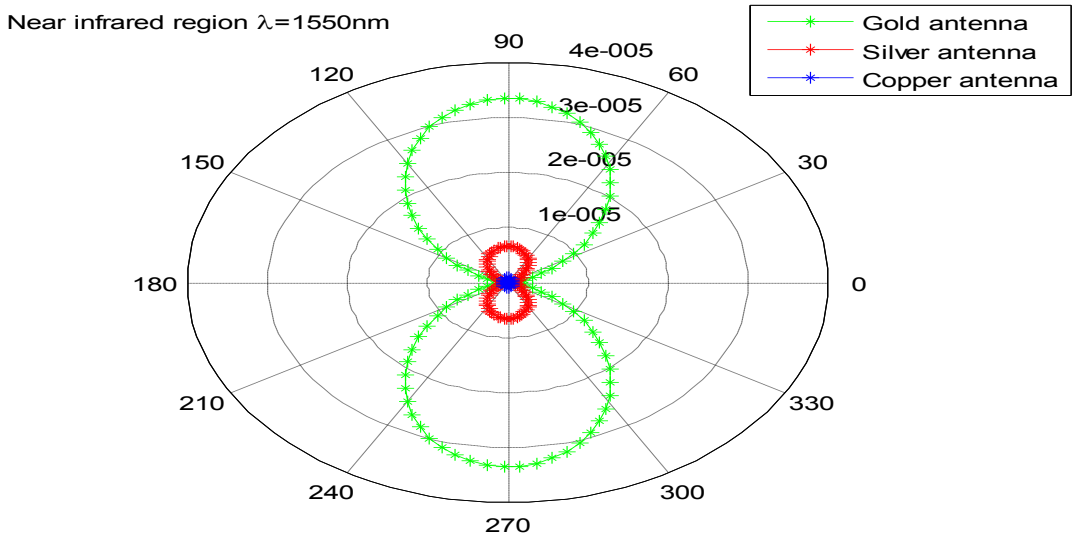

Fig. 36. Antenna radiation pattern intensity in relation to direction angle of electromagnetic waves and different optical antenna types in near infrared transmission region (λ=1550 nm) at the assumed set of the operating parameters.

vii) As shown in Figs. (15-17) have assured that total antenna efficiency for gold, silver and copper antennas increase with increasing its length for different optical transmission regions. As well as in the ultraviolet optical transmission region has presented the highest total antenna efficiency for gold antenna firstly, secondly silver antenna, and finally copper antenna for different antennas under study considerations.

viii) Figs. (18, 19) have demonstrated that maximum power transfer to the antenna increases with increasing antenna thickness and width and decreasing operating optical signal wavelength for different antennas under study considerations. Moreover, it is theoretically found that gold antenna has presented the highest maximum power transfer in comparison with other antennas under the same both antenna dimensions and operating conditions.

ix) As shown in Figs. (20-23) have indicated that return reflection loss (RL) increases with increasing antenna thickness and decreasing antenna length for different antennas under study considerations. It is observed that in the near infrared region around third optical transmission region (λ=1550 nm) has presented the lowest RL for different antenna types under the same operating environments. As well as it is theoretically found that copper antenna has presented the lowest RL in comparison with other antennas under the same both antenna dimensions and operating conditions.

x) Figs. (24, 25) have indicated that antenna radiation intensity increases with increasing both antenna thickness and width and decreasing operating optical signal wavelength for different antenna types. It is found that gold antenna has presented the highest antenna radiation intensity in comparison with other antennas under study at the same operating conditions.

ISSN: 2278 – 909X

xi) Figs. (26-29) have demonstrated that antenna gain increases with increasing antenna length, thickness, and width, in addition to decrease operating optical signal wavelength for different antenna types under the same operating conditions. As well as gold antenna has presented the highest antenna gain in comparison with other antennas under study considerations.

xii) Figs. (30-36) have indicated that gold, silver and copper antennas have maximum its radiation pattern intensity in ultraviolet transmission region in comparison with other optical operating transmission regions. It is observed that gold antenna has presented the maximum radiation intensity pattern in different optical transmission operating regions in comparison with antenna types under the same both antenna dimensions and operating conditions.

V. CONCLUSIONS

In a summary, the model have been investigated to show numerical simulation of different optical dipole antennas in different optical transmission regions. Research in the field of optical antennas is currently driven by the need for high field enhancement, strong field localization, and large absorption cross sections. In one way or another, optical antennas make processes more efficient or increase the specificity of gathered information in the ultra violet, visible and near infrared band regions. It is theoretically found an important effects of the choosing antenna dimensions on its gain, radiation intensity, radiation pattern intensity, antenna efficiency, maximum power transfer, directivity, reflection efficiency, reflection return loss. As well as we have taken in to account to build an equivalent circuit of these antennas of lumped components and estimated its values. Antenna and radiation resistances are the major important parameters for estimating its total antenna efficiency, antenna radiation pattern intensity and antenna gain.

REFERENCES

[1] C. Nehl, H. Liao, and J. H. Hafner, "Optical Properties of Star shaped Gold Micro Particles," Micro. Lett., Vol. 6, pp. 683-688, 2006.

[2] H. Fischer, and O. Martin, "Engineering the Optical Response of Plasmonic Micro Antennas," Opt. Express, Vol. 16, No. 12, pp. 9144-9154, 2008.

[3] F. Kong, K. Li, B. Wu, H. Huang, H. Chen, and J. A. Kong, "Propagation Properties of the SPP Modes in Microscale Narrow Metallic Gap, Channel, and Hole Geometries," Progress In Electromagnetics Research (PIER), Vol. 76, pp. 449-466, 2007.

[4] F. Kong, K. Li, H. Huang, B. Wu, and J. A. Kong, "Analysis of the Surface Magneto Plasmon Modes in the Semiconductor Slit Waveguide at Terahertz Frequencies," Progress In Electromagnetics Research (PIER), Vol. 82, pp. 257-270, 2008.

[5] F. Kong, B. Wu, H. Chen, and J. A. Kong, "Surface Plasmon Mode Analysis of Microscale Metallic Rectangular Waveguide," Opt. Express, Vol. 15, No. 19, pp. 12331-12337, 2007.

[6] L. Blanco, and F. J. Garcia de Abajo, "Spontaneous Light Emission in Complex Microstructures," Phys. Rev. B, Vol. 69, No. 20, pp. 205-214, 2004.

[7] Z. Liu and Y. Bando, "A novel method for preparing copper nanorods and nanowires," Adv. Mater, vol. 15, pp. 303–305, 2003.

[8] P. I. Wang, Y. P. Zhao, G. C. Wang, and T. M. Lu, "Novel growth mechanism of single crystalline Cu nanorods by electron beam irradiation," Nanotechnology, vol. 15, pp. 218–222, 2004.

[9] C. Giradr, "Near fields in nanostructures," Rep. Prog. Phys., vol. 68, pp. 1883–1933, 2005.

[10] J. Alda, J. M. Rico-García, J. M. López, and G. Boreman, "Optical antennas for nano-photonic applications," Nanotechnology, vol. 16, pp. S230–S234, 2005.

[11] C. Fumeaux, J. Alda, and G. D. Boreman, "Lithographic antennas at visible frequencies," Opt. Lett., vol. 24, pp. 1629–1631, 1999.

[12] R. W. P. King and T. T. Wu, "The imperfectly conducting cylindrical transmitting antenna," IEEE Trans. Antennas Propag., vol. AP-14, pp. 524–534, Sep. 1966.

[13] C. D. Taylor, C. W. Harrison, and E. A. Aronson, "Resistive receiving and scattering antenna," IEEE Trans. Antennas Propag., vol. AP-15, pp. 371–376, May 1967.

[14] O. J. F. Martin, C. Girard, and A. Dereux, "Generalized field propagator for electromagnetic scattering and light confinement," Phys. Rev. Lett., vol. 74, pp. 526–529, 1995.

[15] J. C. Weeber, A. Dereux, Ch. Girard, G. C. Des Francs, J. R. Krenn, and J. P. Goudonnet, "Optical addressing at the subwavelength scale," Phys. Rev. E., vol. 62, pp. 7381–7388, 2000.

[16] M. Paulus and O. J. F. Martin, "Light propagation and scattering in stratified media: A Green's tensor approach," Opt. Soc. Amer. A, vol. 18, pp. 854–861, 2001.

[17] T. Søndergaard and B. Tromborg, "Lippmann-Schwinger integral equation approach to the emission of radiation by sources located inside finite-sized dielectric cylinders," Phys. Rev. E, vol. 66, pp. 155309:1–13, 2002.

[18] V. A. Podolskiy, A. K. Sarychev, E. E. Narimanov, and V. M. Shalaev, "Resonant light interaction with plasmonic nanowire systems," J. Opt. A, vol. 7, pp. S32–S37, 2005.

[19] D. P. Fromm, A. Sundaramurthy, P. J. Schuck, G. Kino, and W. E. Moerner, "Gap-dependent optical coupling of single "bowtie" nanoantennas resonant in the visible," Nano Lett., vol. 4, no. 5, pp. 957–961, 2004.

[20] P. J. Schuck, D. P. Fromm, A. Sundaramurthy, G. S. Kino, and W. E. Moerner, "Improving the mismatch between light and nanoscale objects with gold bowtie

ISSN: 2278 – 909X

nanoantennas," Phys. Rev. Lett., vol. 94, pp. 017402:1–4, 2005.
[21] G. W. Hanson, "Fundamental transmitting properties of carbon nanotube antennas," IEEE Trans. Antennas Propag., vol. 53, pp. 3426–3435, Nov. 2005.
[22] W. Steinhögl, G. Schindler, G. Steinlesberger, M. Traving, and M. Engelhardt, "Comprehensive study of the resistivity of copper wires with lateral dimensions of 100 nm and smaller," J. Appl. Phys., vol. 97, pp. 023706:1–7, 2005.

Author's Profile

Dr. Ahmed Nabih Zaki Rashed was born in Menouf city, Menoufia State, Egypt country in 23 July, 1976. Received the B.Sc., M.Sc., and Ph.D. scientific degrees in the Electronics and Electrical Communications Engineering Department from Faculty of Electronic Engineering, Menoufia University in 1999, 2005, and 2010 respectively. Currently, his job carrier is a scientific lecturer in Electronics and Electrical Communications Engineering Department, Faculty of Electronic Engineering, Menoufia university, Menouf. Postal Menouf city code: 32951, EGYPT. His scientific master science thesis has focused on polymer fibers in optical access communication systems. Moreover his scientific Ph. D. thesis has focused on recent applications in linear or nonlinear passive or active in optical networks. His interesting research mainly focuses on transmission capacity, a data rate product and long transmission distances of passive and active optical communication networks, wireless communication, radio over fiber communication systems, and optical network security and management. He has published many high scientific research papers in high quality and technical international journals in the field of advanced communication systems, optoelectronic devices, and passive optical access communication networks. His areas of interest and experience in optical communication systems, advanced optical communication networks, wireless optical access networks, analog communication systems, optical filters and Sensors. As well as he is editorial board member in high academic scientific International research Journals. Moreover he is a reviewer member in high impact scientific research international journals in the field of electronics, electrical communication systems, optoelectronics, information technology and advanced optical communication systems and networks. His personal electronic mail ID (E-mail:ahmed_733@yahoo.com). His published paper under the title **"High reliability optical interconnections for short range applications in high performance optical communication systems"** in Optics and Laser Technology, Elsevier Publisher has achieved most popular download articles in 2013.

ISSN: 2278 – 909X